

# An accurate and robust numerical method for micromagnetics simulations



Darae Jeong, Junseok Kim\*

Department of Mathematics, Korea University, Seoul 136-713, Republic of Korea

## ARTICLE INFO

### Article history:

Received 23 May 2013

Received in revised form

6 December 2013

Accepted 30 December 2013

Available online 16 January 2014

### Keywords:

Micromagnetics simulations

Landau–Lifshitz equation

Finite difference method

Crank–Nicolson scheme

Multigrid method

## ABSTRACT

We propose a new robust, accurate, and fast numerical method for solving the Landau–Lifshitz equation which describes the relaxation process of the magnetization distribution in ferromagnetic material. The proposed numerical method is second-order accurate in both space and time. The approach uses the nonlinear multigrid method for handling the nonlinearities at each time step. We perform numerical experiments to show the efficiency and accuracy of the new algorithm on two- and three-dimensional space. The numerical results show excellent agreements with exact analytical solutions, the second-order accuracy in both space and time, and the energy conservation or dissipation property.

© 2014 Elsevier B.V. All rights reserved.

## 1. Introduction

The Landau–Lifshitz (LL) equation [1] which describes the evolution of the magnetization in a ferromagnetic material [2,3] plays an important role in understanding the mechanisms of magnetization [1,4].

In one-dimensional case, many authors have studied the soliton solution, the interaction of solitary waves, and other properties of the solitary waves [5–7]. Also, the high-dimensional dynamics have been researched in Refs. [8–11].

In this paper, we consider a new robust and accurate numerical method for the Landau–Lifshitz equation with a damping term:

$$\frac{\partial \mathbf{m}(\mathbf{x}, t)}{\partial t} = -\mathbf{m}(\mathbf{x}, t) \times \Delta \mathbf{m}(\mathbf{x}, t) - \mu \mathbf{m}(\mathbf{x}, t) \times [\mathbf{m}(\mathbf{x}, t) \times \Delta \mathbf{m}(\mathbf{x}, t)], \quad (1)$$

where  $\mathbf{m}(\mathbf{x}, t) = (u(\mathbf{x}, t), v(\mathbf{x}, t), w(\mathbf{x}, t))$  is a magnetization vector field for  $\mathbf{x} \in \Omega$  and  $0 < t \leq T$ . Here,  $\mu \geq 0$  is the damping parameter and  $\Omega \subset \mathbb{R}^d$  ( $d = 1, 2, 3$ ) is a domain.

In this paper, we consider the simplified LL equation which is not magnetostatic, anisotropy, and Zeeman field. However, we note that this simplification does not limit the proposed analysis.

Here, we review briefly the properties of the Landau–Lifshitz equation:

- Let  $E(\mathbf{m}(t)) := \int_{\Omega} |\nabla \mathbf{m}(\mathbf{x}, t)|^2 d\mathbf{x}$  be an energy. Here, if  $\mathbf{x} = (x, y, z)$ , then  $|\nabla \mathbf{m}(\mathbf{x}, t)|$  is defined as

$$|\nabla \mathbf{m}(\mathbf{x}, t)| = \sqrt{\left| \frac{\partial \mathbf{m}(\mathbf{x}, t)}{\partial x} \right|^2 + \left| \frac{\partial \mathbf{m}(\mathbf{x}, t)}{\partial y} \right|^2 + \left| \frac{\partial \mathbf{m}(\mathbf{x}, t)}{\partial z} \right|^2},$$

where  $\frac{\partial \mathbf{m}(\mathbf{x}, t)}{\partial x} = \frac{\partial u(\mathbf{x}, t)}{\partial x} \mathbf{i} + \frac{\partial v(\mathbf{x}, t)}{\partial x} \mathbf{j} + \frac{\partial w(\mathbf{x}, t)}{\partial x} \mathbf{k}$ , and so on. To represent it as the other form of energy  $E(\mathbf{m}(t))$ , we take a derivative  $\partial \mathbf{m}/\partial t$  as

$$\frac{\partial E(\mathbf{m}(t))}{\partial t} = \int_{\Omega} \left( 2 \frac{\partial \mathbf{m}}{\partial x} \cdot \frac{\partial^2 \mathbf{m}}{\partial t \partial x} + 2 \frac{\partial \mathbf{m}}{\partial y} \cdot \frac{\partial^2 \mathbf{m}}{\partial t \partial y} + 2 \frac{\partial \mathbf{m}}{\partial z} \cdot \frac{\partial^2 \mathbf{m}}{\partial t \partial z} \right) d\mathbf{x}.$$

Integration by parts using the zero Neumann or periodic boundary conditions gives

\* Corresponding author. Tel.: +82 2 3290 3077; fax: +82 2 929 8562.

E-mail addresses: [cfdkim@korea.ac.kr](mailto:cfdkim@korea.ac.kr), [junseok\\_kim@yahoo.com](mailto:junseok_kim@yahoo.com) (J. Kim).

URL: <http://math.korea.ac.kr/cfdkim>

$$\begin{aligned}
\frac{\partial E(\mathbf{m}(t))}{\partial t} &= \left( 2 \frac{\partial \mathbf{m}}{\partial x} \cdot \frac{\partial \mathbf{m}}{\partial t} + 2 \frac{\partial \mathbf{m}}{\partial y} \cdot \frac{\partial \mathbf{m}}{\partial t} + 2 \frac{\partial \mathbf{m}}{\partial z} \cdot \frac{\partial \mathbf{m}}{\partial t} \right) |_{\partial\Omega} - 2 \int_{\Omega} \left( \frac{\partial^2 \mathbf{m}}{\partial x^2} \cdot \frac{\partial \mathbf{m}}{\partial t} + \frac{\partial^2 \mathbf{m}}{\partial y^2} \cdot \frac{\partial \mathbf{m}}{\partial t} + \frac{\partial^2 \mathbf{m}}{\partial z^2} \cdot \frac{\partial \mathbf{m}}{\partial t} \right) d\mathbf{x} \\
&= -2 \int_{\Omega} \Delta \mathbf{m} \cdot \mathbf{m}_t d\mathbf{x} = 2 \int_{\Omega} \Delta \mathbf{m} \cdot (\mathbf{m} \times \Delta \mathbf{m} + \mu \mathbf{m} \times [\mathbf{m} \times \Delta \mathbf{m}]) d\mathbf{x} = 2 \int_{\Omega} \Delta \mathbf{m} \cdot (\mu \mathbf{m} \times [\mathbf{m} \times \Delta \mathbf{m}]) d\mathbf{x} \\
&= 2 \int_{\Omega} (\mu \mathbf{m} \times [\mathbf{m} \times \Delta \mathbf{m}]) \cdot \Delta \mathbf{m} d\mathbf{x} = 2\mu \int_{\Omega} (\Delta \mathbf{m} \times \mathbf{m}) \cdot (\mathbf{m} \times \Delta \mathbf{m}) d\mathbf{x} = -2\mu \int_{\Omega} (\mathbf{m} \times \Delta \mathbf{m}) \cdot (\mathbf{m} \times \Delta \mathbf{m}) d\mathbf{x} = -2\mu \int_{\Omega} |\mathbf{m} \times \Delta \mathbf{m}|^2 d\mathbf{x}.
\end{aligned}$$

By integration, we obtain the following energy equation

$$E(\mathbf{m}(t)) = E(\mathbf{m}(0)) - 2\mu \int_0^t \int_{\Omega} |\mathbf{m}(\mathbf{x}, s) \times \Delta \mathbf{m}(\mathbf{x}, s)|^2 d\mathbf{x} ds \quad (2)$$

for any  $t > 0$ . Equation (2) implies that this problem has energy dissipation property for the case  $\mu > 0$  and energy conservation property for the case  $\mu = 0$ .

- Equation (1) has length-preserving property, i.e.,  $|\mathbf{m}(\mathbf{x}, t)| = |\mathbf{m}(\mathbf{x}, 0)|$  for any  $t > 0$ . To show this, we do scalar multiplication of Equation (1) with  $\mathbf{m}$ ,

$$\frac{\partial \mathbf{m}}{\partial t} \cdot \mathbf{m} = -(\mathbf{m} \times \Delta \mathbf{m}) \cdot \mathbf{m} - \mu \mathbf{m} \times (\mathbf{m} \times \mathbf{m}) \cdot \mathbf{m} = 0.$$

Then,  $\partial |\mathbf{m}|^2 / \partial t = 0$ , which implies  $|\mathbf{m}(\mathbf{x}, t)|$  is constant for all  $t$  and each  $\mathbf{x}$ , that is,  $|\mathbf{m}(\mathbf{x}, t)| = |\mathbf{m}(\mathbf{x}, 0)|$ . And we assume that  $|\mathbf{m}(\mathbf{x}, 0)| = 1$ . For a more detailed discussion of the model, see survey articles [12–18].

Numerical method has become an important tool in the study of dynamics of ferromagnetic materials [19–22].

Since explicit methods cause severe time step restriction for stability [23], several methods such as the semi-analytical schemes [23,24] and the high order Runge–Kutta algorithms [25] have been proposed to improve their efficiency. A geometric integration technique based on Cayley transform is applied to the time discretization of the LLG equation [26].

Through the finite element procedure [27–29], numerical solutions are obtained by the extrapolation formula leading to semi-implicit [27,29]. Otherwise, iterative techniques, as fixed-point [30] and quasi-Newton algorithms [31], are needed.

The midpoint rule time discretization technique was applied to Landau–Lifshitz–Gilbert equation [31]. The Gauss–Seidel projection method (GSPM) was introduced by Wang et al. [32] and the improved GSPM was presented by Garcia–Cervera and Weinan [33]. A successive over relaxation method was presented for the LLG [34].

Jeong and Kim [35] suggested a Crank–Nicolson scheme which is accurate, however, it uses an updated source term and repeatedly performed iterations until the numerical solution converges. In this paper, we propose a new robust fast accurate numerical method for computations of the LL equation. The proposed method does not need an updated source term and therefore it is fast. We also perform three-dimensional space experiments.

The contents of this paper are as follows. In Section 2, we describe the discrete semi-implicit finite difference scheme of the Landau–Lifshitz equation. Numerical experiments such as a second-order convergence test and an energy conservation

property of the proposed scheme are given in Section 3. In Section 5, conclusions are drawn.

## 2. Numerical solution

For simplicity of exposition, we shall first discretize the LL equation in one dimensional domain  $\Omega = (0,1)$  with a uniform grid with the number of grid points  $N_x$ , a space step  $h = 1/N_x$ , and a time step  $\Delta t = T/N_t$ . Let us denote the numerical approximation of the solution by

$$\mathbf{m}_i^n = \mathbf{m}(x_i, t^n) = (u_i^n, v_i^n, w_i^n) \approx \begin{pmatrix} u((i-0.5)h, n\Delta t) \\ v((i-0.5)h, n\Delta t) \\ w((i-0.5)h, n\Delta t) \end{pmatrix}^T,$$

where  $i = 1, \dots, N_x$  and  $n = 0, 1, \dots, N_t$ . Let the discrete Laplacian operator be defined as  $\Delta_h \mathbf{m}_i = (\mathbf{m}_{i+1} - 2\mathbf{m}_i + \mathbf{m}_{i-1})/h^2$ . Then the second-order Crank–Nicolson scheme is given as

$$\begin{aligned}
\frac{\mathbf{m}_i^{n+1} - \mathbf{m}_i^n}{\Delta t} &= -\frac{1}{2} \left( \mathbf{m}_i^{n+1} \times \Delta_h \mathbf{m}_i^{n+1} + \mathbf{m}_i^n \times \Delta_h \mathbf{m}_i^n \right) \\
&\quad - \frac{\mu}{2} \left[ \mathbf{m}_i^{n+1} \times \left( \mathbf{m}_i^{n+1} \times \Delta_h \mathbf{m}_i^{n+1} \right) + \mathbf{m}_i^n \times \left( \mathbf{m}_i^n \times \Delta_h \mathbf{m}_i^n \right) \right].
\end{aligned} \quad (3)$$

We use an accurate and fast nonlinear multigrid method [36,37] for solving the resulting discrete system of Eq. (3). To condense the discussion we describe only the relaxation step in the multigrid method since it is the key step in the algorithm. First, let us rewrite Eq. (3) as

$$\mathbf{m}^{n+1} + \frac{\Delta t}{2} (\mathbf{m} \times \Delta_h \mathbf{m})^{n+1} + \frac{\Delta t}{2} \mu [\mathbf{m} \times (\mathbf{m} \times \Delta_h \mathbf{m})]^{n+1} = \phi^n, \quad (4)$$

where

$$\phi^n = \mathbf{m}^n - \frac{\Delta t}{2} (\mathbf{m} \times \Delta_h \mathbf{m})^n - \frac{\Delta t}{2} \mu [\mathbf{m} \times (\mathbf{m} \times \Delta_h \mathbf{m})]^n.$$

In its component form, Eq. (4) becomes

$$\begin{aligned}
\begin{pmatrix} u_i^{n+1} \\ v_i^{n+1} \\ w_i^{n+1} \end{pmatrix} &+ \frac{\Delta t}{2} \begin{pmatrix} v_i \Delta_h w_i - w_i \Delta_h v_i \\ w_i \Delta_h u_i - u_i \Delta_h w_i \\ u_i \Delta_h v_i - v_i \Delta_h u_i \end{pmatrix}^{n+1} \\
&+ \frac{\Delta t}{2} \mu \begin{pmatrix} v_i(u_i \Delta_h v_i - v_i \Delta_h u_i) - w_i(w_i \Delta_h u_i - u_i \Delta_h w_i) \\ w_i(w_i \Delta_h w_i - w_i \Delta_h v_i) - u_i(u_i \Delta_h v_i - v_i \Delta_h u_i) \\ u_i(w_i \Delta_h u_i - u_i \Delta_h w_i) - v_i(v_i \Delta_h w_i - w_i \Delta_h v_i) \end{pmatrix}^{n+1} = \phi_i^n
\end{aligned} \quad (5)$$

**Table 1**

Maximum norms  $\|\mathbf{e}^n\|_\infty$  of the errors and convergence rates with space step  $h = 1/N_x$ , time step  $\Delta t = 0.32$  h, total time  $T = 0.01$ ,  $\alpha = \pi/12$ ,  $k = 2\pi$ , and a convergence tolerance of 1.0E-10.

Case	$64^2$	Rate	$128^2$	Rate	$256^2$	Rate	$512^2$	Rate	$1024^2$
$\mu = 0.01$	2.4E-3	1.98	6.3E-4	1.99	1.6E-4	2.00	4.0E-5	2.00	9.9E-6
$\mu = 0.1$	2.4E-3	1.98	6.0E-4	1.99	1.5E-4	2.00	3.8E-5	2.00	9.4E-6
$\mu = 0.2$	2.3E-3	1.98	5.8E-4	1.99	1.5E-4	2.00	3.7E-5	2.00	9.2E-6
$\mu = 0.5$	2.4E-3	1.99	6.0E-4	2.00	1.5E-4	2.00	3.8E-5	2.00	9.4E-6
$\mu = 0.9$	2.9E-3	2.00	7.3E-4	2.00	1.8E-4	2.00	4.6E-5	2.00	1.1E-5

for  $i = 1, \dots, N_x$ . Note that

$$\begin{aligned} v_i \Delta_h w_i - w_i \Delta_h v_i &= v_i \frac{w_{i-1} - 2w_i + w_{i+1}}{h^2} - w_i \frac{v_{i-1} - 2v_i + v_{i+1}}{h^2} \\ &= v_i \tilde{\Delta}_h w_i - w_i \tilde{\Delta}_h v_i \quad \text{for } i = 1, \dots, N_x, \end{aligned} \quad (6)$$

where  $\tilde{\Delta}_h w_i = (w_{i-1} + w_{i+1})/h^2$ . This cancellation stabilizes the scheme. By using Eq. (6), we rewrite Eq. (5).

$$A_i \begin{pmatrix} u_i^{n+1} \\ v_i^{n+1} \\ w_i^{n+1} \end{pmatrix} = \phi_i^n, \quad A_i = \begin{pmatrix} a_{11} & a_{12} & a_{13} \\ a_{21} & a_{22} & a_{23} \\ a_{31} & a_{32} & a_{33} \end{pmatrix},$$

where

$$\begin{aligned} a_{11} &= 1 + 0.5\Delta t \mu \left( v_i^{n+1} \tilde{\Delta}_h v_i^{n+1} + w_i^{n+1} \tilde{\Delta}_h w_i^{n+1} \right), \\ a_{12} &= 0.5\Delta t \left( \tilde{\Delta}_h w_i^{n+1} - \mu v_i^{n+1} \tilde{\Delta}_h v_i^{n+1} \right), \\ a_{13} &= -0.5\Delta t \left( \tilde{\Delta}_h v_i^{n+1} + \mu w_i^{n+1} \tilde{\Delta}_h w_i^{n+1} \right), \\ a_{21} &= -0.5\Delta t \left( \tilde{\Delta}_h w_i^{n+1} + \mu u_i^{n+1} \tilde{\Delta}_h v_i^{n+1} \right), \\ a_{22} &= 1 + 0.5\Delta t \mu \left( w_i^{n+1} \tilde{\Delta}_h w_i^{n+1} + u_i^{n+1} \tilde{\Delta}_h u_i^{n+1} \right), \\ a_{23} &= 0.5\Delta t \left( \tilde{\Delta}_h u_i^{n+1} - \mu w_i^{n+1} \tilde{\Delta}_h v_i^{n+1} \right), \\ a_{31} &= 0.5\Delta t \left( \tilde{\Delta}_h v_i^{n+1} - \mu u_i^{n+1} \tilde{\Delta}_h w_i^{n+1} \right), \\ a_{32} &= -0.5\Delta t \left( \tilde{\Delta}_h u_i^{n+1} + \mu v_i^{n+1} \tilde{\Delta}_h w_i^{n+1} \right), \\ a_{33} &= 1 + 0.5\Delta t \mu \left( u_i^{n+1} \tilde{\Delta}_h u_i^{n+1} + v_i^{n+1} \tilde{\Delta}_h v_i^{n+1} \right). \end{aligned}$$

Then using  $3 \times 3$  matrix inversion, the iteration solution is given as

$$(u_i^{n+1}, v_i^{n+1}, w_i^{n+1}) = A_i^{-1} \phi_i^n \quad \text{for } i = 1, \dots, N_x,$$

where we use a Gauss–Seidel type update for evaluation of  $A_i$ . For the detailed description of a multigrid algorithm, see Refs. [35,38].

### 3. Numerical experiments

In this section we validate the proposed numerical scheme by verifying the second-order convergence in both space and time.

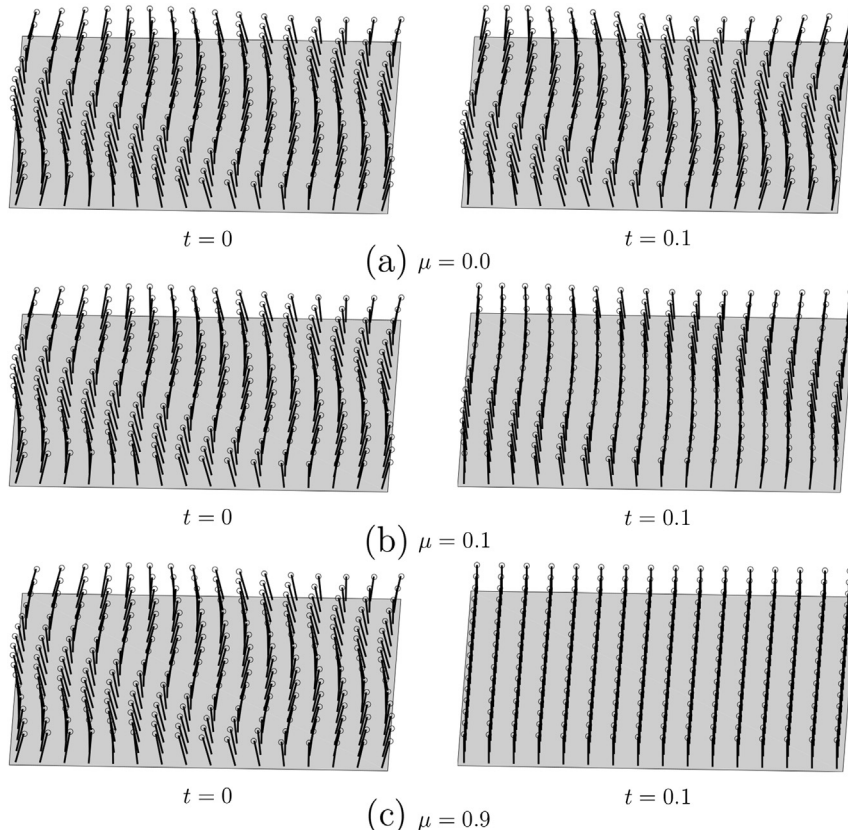


**Fig. 1.** Snapshots of the magnetization pattern with (a)  $\mu = 0.0$ , (b)  $\mu = 0.1$ , and (c)  $\mu = 0.9$ . Initial vector field (left row) and numerical solutions (right row) at  $T = 0.1$  with spatial step  $h = 1/64$ , temporal step  $\Delta t = 0.005$ ,  $\alpha = \pi/12$ ,  $k = 2\pi$ , and a convergence tolerance of 1.0E-10.

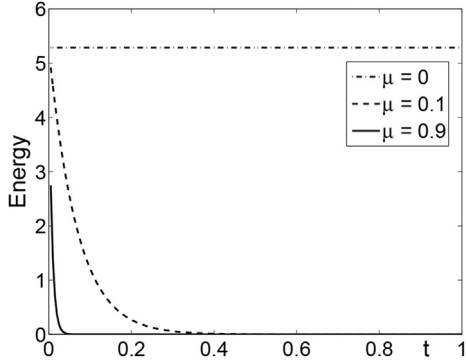


**Fig. 2.** A temporal evolution of the discrete energy of the numerical solution with (a)  $\mu = 0$ , (b)  $\mu = 0.1$ , and (c)  $\mu = 0.9$ .

And we show that time evolution of  $\mathbf{m}$  and energy property with different  $\mu$ .

### 3.1. Exact solutions

Before starting several numerical simulations, we present non-trivial exact solutions [13] for Landau–Lifshitz equation (1) on  $\Omega$  with a periodic boundary condition with respect to dimension. Here, let  $\alpha \in \mathbb{R}$ ,  $l \in \mathbb{Z}$ , and  $k = l\pi$ .

#### 3.1.1. Exact solution in two dimension

The exact solution  $\mathbf{m}^e(x, y, t)$  in two dimension is given by

$$\begin{aligned} u^e(x, y, t) &= \sin\alpha\cos[k(x + y) + g(t)]/d(t), \\ v^e(x, y, t) &= \sin\alpha\sin[k(x + y) + g(t)]/d(t), \\ w^e(x, y, t) &= e^{2k^2\mu t}\cos\alpha/d(t), \end{aligned}$$

**Table 2**

Maximum norms  $\|\mathbf{e}^n\|_\infty$  of the errors and convergence rates with space step  $h = 1/N_x$ , time step  $\Delta t = 0.32$  h, total time  $T = 0.1$ ,  $\alpha = \pi/24$ ,  $k = 2\pi$ , and a convergence tolerance of 1.0E-6.

Case	$32^2$	Rate	$64^2$	Rate	$128^2$
$\mu = 0.01$	1.28E-1	1.74	3.84E-2	1.94	9.97E-3
$\mu = 0.1$	5.25E-2	1.89	1.42E-2	1.99	3.56E-3
$\mu = 0.2$	1.98E-2	2.07	4.77E-3	2.04	1.15E-3
$\mu = 0.5$	3.64E-3	1.99	9.17E-4	2.00	2.29E-4
$\mu = 0.9$	5.27E-3	1.99	1.33E-3	2.01	3.30E-4

where

$$d(t) = \sqrt{\sin^2\alpha + e^{4k^2\mu t}\cos^2\alpha}, \quad g(t) = \frac{1}{\mu} \log\left(\frac{d(t) + e^{2k^2\mu t}\cos\alpha}{1 + \cos\alpha}\right).$$

#### 3.1.2. Exact solution in three dimension

The exact solution  $\mathbf{m}^e(x, y, z, t)$  in three dimension is given by

$$\begin{aligned} u^e(x, y, z, t) &= \sin\alpha\cos[k(x + y + z) + g(t)]/d(t), \\ v^e(x, y, z, t) &= \sin\alpha\sin[k(x + y + z) + g(t)]/d(t), \\ w^e(x, y, z, t) &= e^{3k^2\mu t}\cos\alpha/d(t), \end{aligned}$$

where

$$d(t) = \sqrt{\sin^2\alpha + e^{6k^2\mu t}\cos^2\alpha}, \quad g(t) = \frac{1}{\mu} \log\left(\frac{d(t) + e^{3k^2\mu t}\cos\alpha}{1 + \cos\alpha}\right).$$

### 3.2. Two-dimensional space

Now, we consider Eq. (1) on the two-dimensional unit domain. And for the numerical test, we apply an initial condition  $(u^e(x, y, 0), v^e(x, y, 0), w^e(x, y, 0))$  as

$$u^e(x, y, 0) = \sin\alpha\cos[k(x + y)], \quad (7)$$

$$v^e(x, y, 0) = \sin\alpha\sin[k(x + y)], \quad (8)$$

$$w^e(x, y, 0) = \cos\alpha, \quad (9)$$

and a periodic boundary condition.

#### 3.2.1. Convergence test

**Table 1** shows the maximum norms of the errors and convergence rates with space step  $h = 1/N_x$ , time step  $\Delta t = 0.32$  h, total time  $T = 0.1$ ,  $\alpha = \pi/24$ ,  $k = 2\pi$ , and a convergence tolerance of 1.0E-10. Parameter values are  $\alpha = \pi/12$  and  $k = 2\pi$ . The results suggest that the scheme is second-order accurate in space and time.

#### 3.2.2. Time evolution

**Fig. 1** shows the vector field  $0.1\mathbf{m}$  of the numerical solution at (a)  $T = 0$  and (b)  $T = 0.1$ . We observe that the solution at  $T = 0.1$  is a translation of the initial configuration without changing its magnitude. Here we scaled  $\mathbf{m}$  as  $0.1\mathbf{m}$  for a visual clarity.

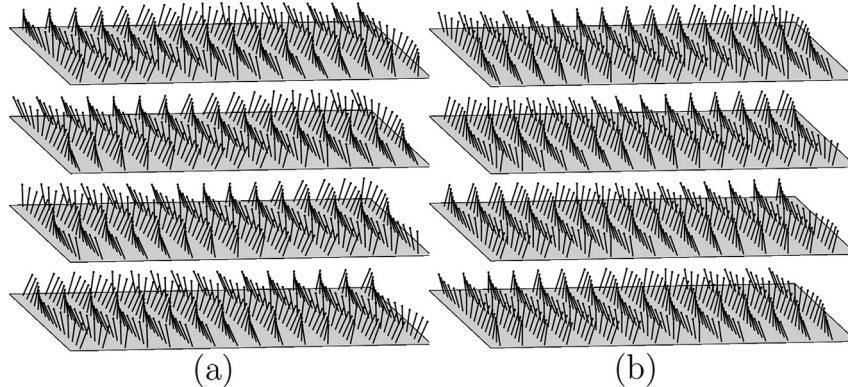


**Fig. 3.** Snapshots of the magnetization pattern on 3D. (a) Initial vector field and (b) numerical solution at  $T = 0.2$  with space step  $h = 1/32$ , time step  $\Delta t = 0.32$  h,  $\alpha = \pi/24$ ,  $k = 2\pi$ , and a convergence tolerance of 1.0E-6.

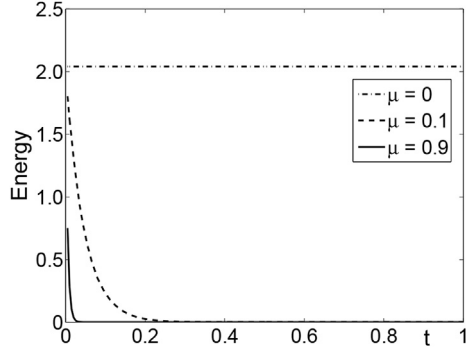


**Fig. 4.** A temporal evolution of the discrete energy of the numerical solution with (a)  $\mu = 0$ , (b)  $\mu = 0.1$ , and (c)  $\mu = 0.9$ .

### 3.2.3. Energy property

Next, to test an energy property, we define a discrete energy as

$$E(\mathbf{m}^n) = \sum_{i=1}^{N_x} \sum_{j=1}^{N_y} \left[ (u_{i+1,j}^n - u_{ij}^n)^2 + (v_{i+1,j}^n - v_{ij}^n)^2 + (w_{i+1,j}^n - w_{ij}^n)^2 + (u_{ij+1}^n - u_{ij}^n)^2 + (v_{ij+1}^n - v_{ij}^n)^2 + (w_{ij+1}^n - w_{ij}^n)^2 \right].$$

**Fig. 2** shows the time evolution of the energy  $E(\mathbf{m}^n)$  with  $N_x = N_y = 64$  up to time  $T = 1$  in three cases  $\mu = 0, 0.1$ , and  $0.9$ .

As expected from the energy equation (2) of the governing model, the conservation of energy holds when  $\mu = 0$ . And in the other case with  $\mu = 0.1$  and  $0.9$ , we can see that the energy dissipates during the time evolution.

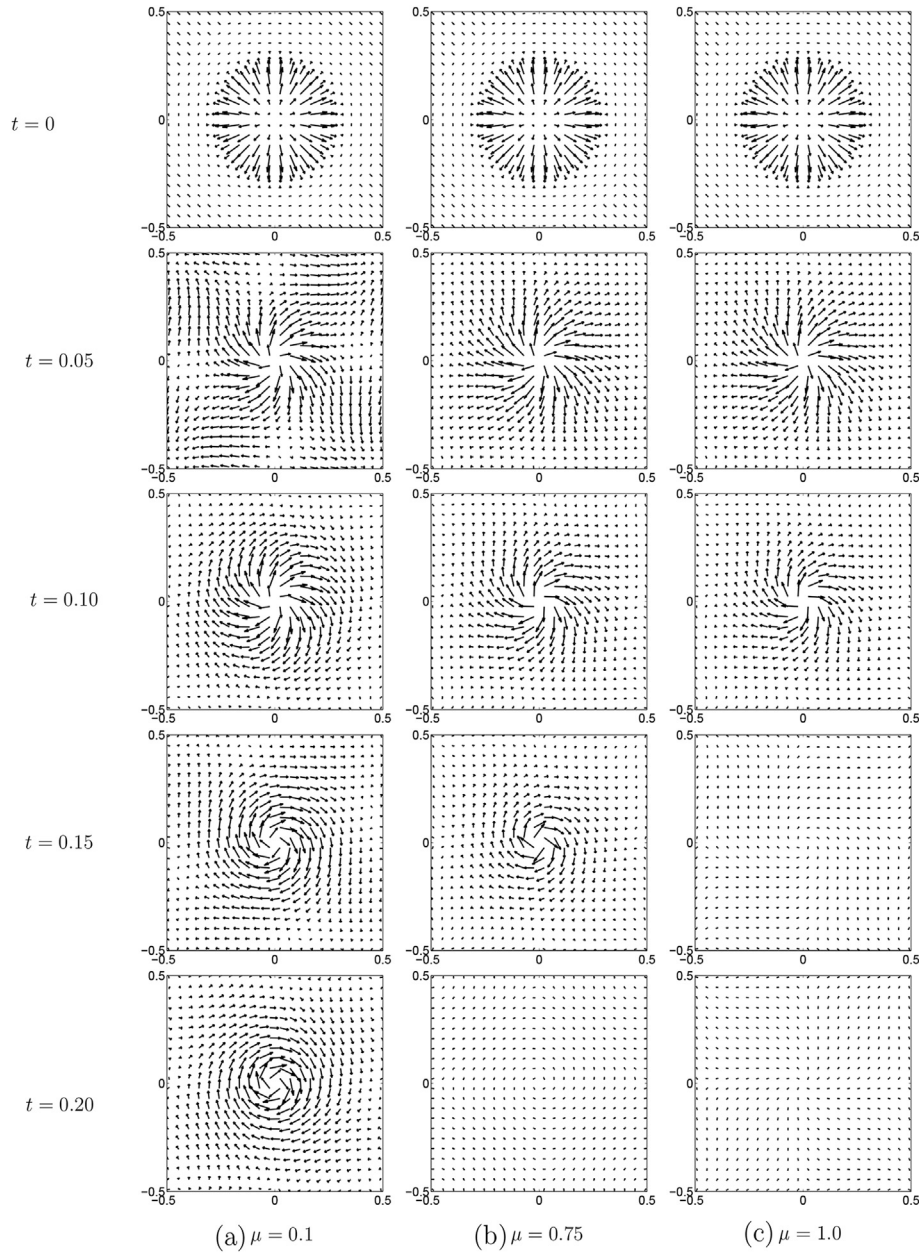


**Fig. 5.** Time evolution of numerical approximation  $\mathbf{m}(t)$  with  $h = 1/64$ ,  $\Delta t = 0.1/64^2$  for (a)  $\mu = 0.1$ , (b)  $\mu = 0.5$ , and (c)  $\mu = 1$  at  $t = 0, 0.05, 0.1, 0.15$ , and  $0.2$ . For visualization, we only plot vector field  $(u, v)$ .

### 3.3. Three-dimensional space

In this section, the three-dimensional equation on  $\Omega = (0,1) \times (0,1) \times (0,1)$  with periodic boundary conditions is considered. And we apply an initial condition as  $(u^e(x, y, z, 0), v^e(x, y, z, 0), w^e(x, y, z, 0))$ .

#### 3.3.1. Convergence test

We perform three-dimensional numerical experiments with exact solutions to verify the second-order accuracy of the proposed scheme in space and time. In Table 2, the results represent the maximum norms of the errors and convergence rates for  $\mathbf{m}$  of the scheme with space step  $h = 1/N_x$ , time step  $\Delta t = 0.32$  h, total time  $T = 0.1$ ,  $\alpha = \pi/24$ ,  $k = 2\pi$ , and a convergence tolerance of 1.0E-6. The results suggest that the scheme is indeed second-order accurate in space and time.

#### 3.3.2. Time evolution

Fig. 3 shows the vector field  $0.1\mathbf{m}$  of the numerical solution on 3D at (a)  $T = 0$  and (b)  $T = 0.2$ . We observe that the initial configuration is translated to the numerical solution at  $T = 0.2$  with same magnitude.

#### 3.3.3. Energy property

We define a discrete energy as

$$\begin{aligned} E(\mathbf{m}^n) = h \sum_{i=1}^{N_x} \sum_{j=1}^{N_y} \sum_{k=1}^{N_z} & \left[ \left( u_{i+1,jk}^n - u_{ijk}^n \right)^2 + \left( v_{i+1,jk}^n - v_{ijk}^n \right)^2 + \left( w_{i+1,jk}^n - w_{ijk}^n \right)^2 + \left( u_{i,j+1,k}^n - u_{ijk}^n \right)^2 + \left( v_{i,j+1,k}^n - v_{ijk}^n \right)^2 \right. \\ & \left. + \left( w_{i,j+1,k}^n - w_{ijk}^n \right)^2 + \left( u_{ij,k+1}^n - u_{ijk}^n \right)^2 + \left( v_{ij,k+1}^n - v_{ijk}^n \right)^2 + \left( w_{ij,k+1}^n - w_{ijk}^n \right)^2 \right]. \end{aligned}$$

Theoretically, the energy is constant irrespective of time when  $\mu = 0$  and the energy decay when  $\mu > 0$  as time goes by. Now we

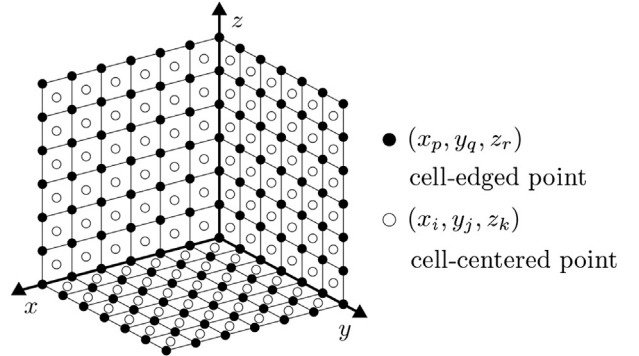


Fig. 7. Two adjacent different points  $(x_p, y_q, z_r)$  and  $(x_i, y_j, z_k)$  used in Eq. (14).

confirm that numerically. Fig. 4 shows the time evolution of the energy  $E(\mathbf{m}^n)$  with  $N_x = N_y = N_z = 32$  up to time  $T = 0.1$  with three different  $\mu$ . When  $\mu = 0$ , we can check that the energy is conserved regardless of time. However, when  $\mu$  is nonzero value, the energy decreases with time  $t$ .

#### 3.4. Finite-time blow-up solutions and geometric changes

We present the numerical performance of our proposed scheme in some numerical example given in Refs. [39,40] and study finite

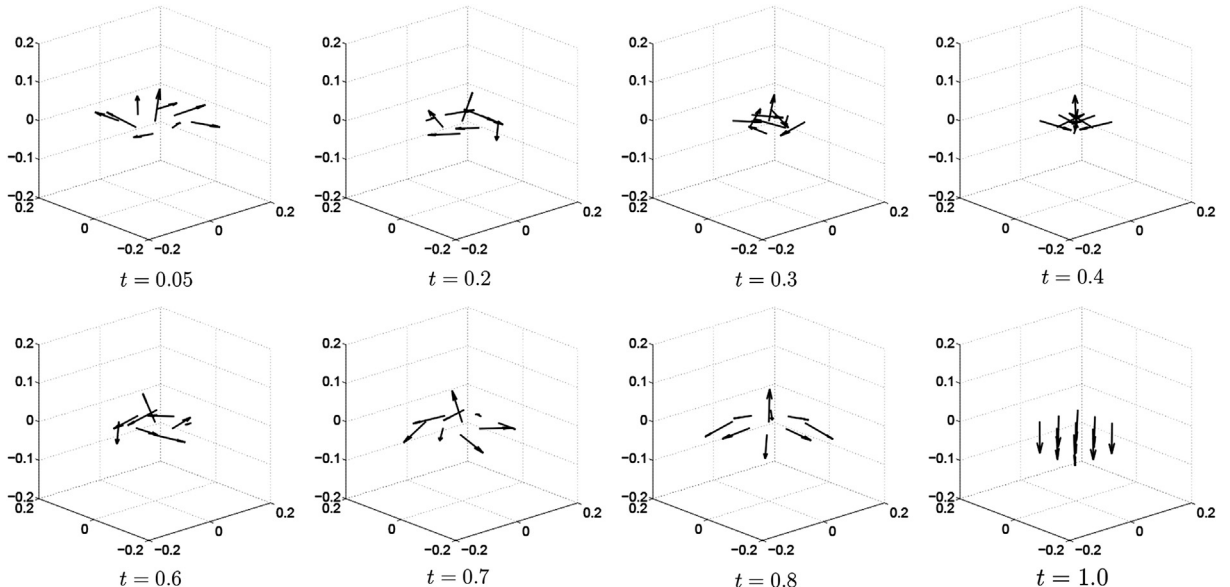
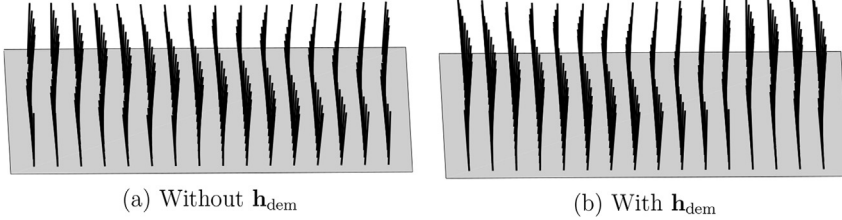


Fig. 6. Nodal values of numerical approximation  $\mathbf{m}(t)$  for nodes  $(x, y)$  close to the origin with  $h = 1/64$ ,  $\Delta t = 1.0/64^2$  for  $\mu = 0.1$  as time goes on.

blow-up of weak solutions. Let  $\Omega = (-1/2, 1/2) \times (-1/2, 1/2)$  and let  $\mathbf{m}_0: \Omega \rightarrow S^2$  be defined by



**Fig. 8.** Snapshots of the magnetization pattern on  $z = 0.4$  (a) with  $\mathbf{h}_{\text{dem}}$  and (b) without  $\mathbf{h}_{\text{dem}}$  at  $T = 0.5$ . Here, the following parameters are used:  $h = 1/16$ ,  $\Delta t = 0.02$ ,  $\mu = 0.01$ ,  $M_d = 1.0$ ,  $\Omega = (0, 1) \times (0, 1) \times (0, 1)$ .

$$\mathbf{m}_0(\mathbf{x}) = \begin{cases} (0, 0, -1) & \text{if } |\mathbf{x}| \geq 1/2, \\ (2A\mathbf{x}, A^2 - |\mathbf{x}|^2) / (A^2 + |\mathbf{x}|^2) & \text{if } |\mathbf{x}| < 1/2, \end{cases}$$

where  $A = (1 - 2|\mathbf{x}|)^4$  and  $\mathbf{x} = (x, y) \in \Omega$ .

Fig. 5 shows snapshots of the numerical solution  $\mathbf{m}$  for different  $\mu$  at various times. In this figure, we observe that numerical solutions with  $\mu = 0.1, 0.75, 1.0$  have a similar behavior. But the larger the value of  $\mu$  is, the faster the numerical solution happens blow-up.

Next Fig. 6 represents the nodal values of numerical approximation  $\mathbf{m}(t)$  for nodes  $(x, y)$  close to the origin with  $h = 1/64$ ,  $\Delta t = 0.1/64^2$  for  $\mu = 0.1$  as time goes on. At  $t = 1.0$ , we can observe that the vector at the origin changes its direction from  $(0, 0, 1)$  to  $(0, 0, -1)$ . Such views represent blow-up occurrences.

#### 4. Effect of the magnetostatic field

We propose the method to treat the magnetostatic vector field for  $\mathbf{x} = (x, y, z)$  on  $\Omega \subset \mathbb{R}^3$ . First, we consider the following governing equations:

$$\frac{\partial \mathbf{m}(\mathbf{x}, t)}{\partial t} = -\mathbf{m}(\mathbf{x}, t) \times (\mathbf{h}_{\text{ex}}(\mathbf{x}, t) + \mathbf{h}_{\text{dem}}(\mathbf{x}, t)) - \mu \mathbf{m}(\mathbf{x}, t) \times [\mathbf{m}(\mathbf{x}, t) \times (\mathbf{h}_{\text{ex}}(\mathbf{x}, t) + \mathbf{h}_{\text{dem}}(\mathbf{x}, t))], \quad (10)$$

where the exchange field  $\mathbf{h}_{\text{ex}}$  is defined by  $\mathbf{h}_{\text{ex}} = \Delta \mathbf{m}(\mathbf{x}, t)$  and the magnetostatic field  $\mathbf{h}_{\text{dem}}$  is defined by

$$\mathbf{h}_{\text{dem}} = -\frac{M_d}{4\pi} \nabla_{\mathbf{x}} \int_{\Omega} \nabla_{\mathbf{x}'} \left( \frac{1}{|\mathbf{x} - \mathbf{x}'|} \right) \cdot \mathbf{m}(\mathbf{x}', t) dV_{\mathbf{x}'}, \quad (11)$$

where  $M_d$  is constant value.

To solve Eq. (10), we deal with the magnetostatic field  $\mathbf{h}_{\text{dem}}$  explicitly and the other terms by Crank–Nicolson scheme as follows.

$$\begin{aligned} \frac{\mathbf{m}^{n+1} - \mathbf{m}^n}{\Delta t} &= -\frac{1}{2} (\mathbf{m}^{n+1} \times \mathbf{h}_{\text{ex}}^{n+1} + \mathbf{m}^n \times \mathbf{h}_{\text{ex}}^n) - \mathbf{m}^n \times \mathbf{h}_{\text{dem}}^n \\ &\quad - \frac{\mu}{2} [\mathbf{m}^{n+1} \times (\mathbf{m}^{n+1} \times \mathbf{h}_{\text{ex}}^{n+1}) + \mathbf{m}^n \times (\mathbf{m}^n \times \mathbf{h}_{\text{ex}}^n)] \\ &\quad - \mu \mathbf{m}^n \times (\mathbf{m}^n \times \mathbf{h}_{\text{dem}}^n). \end{aligned} \quad (12)$$

To avoid the singularity problem which is occurred in  $\mathbf{h}_{\text{dem}}^n$ , we propose the shifting method. The proposed shifted method is to use the two adjacent different points (See Fig. 7) for calculating Eq. (13). That is,

$$\mathbf{h}_{\text{dem}}^n = -\frac{M_d}{4\pi} \nabla_{\mathbf{x}} \mathbf{H}^n, \quad (13)$$

where

$$\begin{aligned} \mathbf{H}_{pqr}^n &= h^3 \sum_i \sum_j \sum_k \frac{(x_p - x_i, y_q - y_j, z_r - z_k)}{\left[ (x_p - x_i)^2 + (y_q - y_j)^2 + (z_r - z_k)^2 \right]^{\frac{3}{2}}} \\ &\quad \cdot \mathbf{m}^n(x_i, y_j, z_k). \end{aligned} \quad (14)$$

Here, we use two different positions which are denoted by  $(x_p, y_q, z_r)$  and  $(x_i, y_j, z_k)$  to avoid the singularity. As shown in Fig. 7,  $(x_i, y_j, z_k)$  is cell-centered point which is defined as  $x_i = (i + 0.5)h$ ,  $y_j = (j + 0.5)h$ ,  $z_k = (k + 0.5)h$  and  $(x_p, y_q, z_r)$  is cell-edged point which is defined as  $x_p = ph$ ,  $y_q = qh$ ,  $z_r = rh$ .

By using the proposed shifting method, we can get numerical solution of Eq. (13). The following figure represents the numerical solution of Eq. (10). In this test, we use the following parameters:  $h = 1/16$ ,  $\Delta t = 0.02$ ,  $\mu = 0.01$ ,  $M_d = 1.0$ ,  $\Omega = (0, 1) \times (0, 1) \times (0, 1)$ . And the initial condition is used by Eqs. (7)–(9). To show the effect of term  $\mathbf{h}_{\text{dem}}^n$ , we plot the snapshots of the magnetization pattern on  $z = 0.4$  with  $\mathbf{h}_{\text{dem}}$  and without  $\mathbf{h}_{\text{dem}}$  at  $T = 0.5$ , respectively (Fig. 8).

#### 5. Conclusion

In this paper, we have proposed a new robust, accurate, and fast numerical method for the Landau–Lifshitz equation which describes a great variety of the evolution of magnetization patterns in ferromagnetic media. We validated the second-order accuracy of the proposed method in both space and time. We performed two- and three-dimensional numerical experiments to show the efficiency and accuracy of the new algorithm. The numerical results showed excellent agreement with exact analytical solutions.

#### Acknowledgments

This work was supported by a Korea University Grant. The first author (D. Jeong) and the corresponding author (J.S. Kim) greatly appreciate the reviewers for their constructive comments and suggestions, which improved the quality of this paper.

#### References

- [1] L. Landau, E. Lifshitz, Phys. Zeitsch. der Sow. 8 (1935) 153–169.
- [2] S.J. Kim, W. Kim, S.H. Bae, C.S. Kim, J. Yoon, M.H. Jung, K.J. Kim, J. Korean Phys. Soc. 52 (2) (2008) 492–495.
- [3] S.K. Sharma, M. Knobel, C.T. Meneses, S. Kumar, Y.J. Kim, B.H. Koo, C.G. Lee, D.K. Shukla, R. Kumar, J. Korean Phys. Soc. 55 (3) (2009) 1018–1021.
- [4] W.F. Brown, *Micromagnetics*, Wiley, New York, 1963.
- [5] K. Nakamura, T. Sasada, Phys. Lett. A 48 (5) (1974) 321–322.
- [6] M. Lakshmanan, T.W. Ruijgrok, C.J. Thompson, Phys. A 84 (3) (1976) 577–590.

- [7] P.-L. Sulem, C. Sulem, C. Bardos, *Commun. Math. Phys.* 107 (3) (1986) 431–454.
- [8] B. Guo, G. Yang, *J. Math. Phys.* 42 (11) (2001) 5223–5227.
- [9] L.D. Buda, I.L. Prejbeanu, U. Ebels, K. Ounadjela, *J. Magn. Magn. Mater.* 242–248 (2) (2002) 996–998.
- [10] G. Yang, B. Guo, *Nonlinear Anal.-Theor.* 71 (9) (2009) 3999–4006.
- [11] P. Zhong, S. Wang, K. Wang, Y. Bai, *Discrete Dyn. Nat. Soc.* 2010 (2010) 1–13.
- [12] M. Kružík, A. Prohl, *SIAM Rev.* 48 (3) (2005) 439–483.
- [13] A. Fuwa, T. Ishiwata, M. Tsutsumi, Finite difference scheme for the Landau–Lifshitz equation, in: Proc. Czech-Japanese Seminar in Appl. Math., September 14–17, 2006, pp. 107–113.
- [14] I. Cimrák, *Arch. Comput. Meth. Eng.* 15 (2007) 1–37.
- [15] D. Seddaoui, S. Loranger, M. Malatek, D. Ménard, A. Yelon, *IEEE Trans. Magn.* 47 (2) (2011) 279–283.
- [16] X. Wang, K. Gao, M. Seigler, *IEEE Trans. Magn.* 47 (10) (2011) 2676–2679.
- [17] C. Ragusa, M. d'Aquino, C. Serpico, B. Xie, M. Repetto, G. Bertotti, D. Ansalone, *IEEE Trans. Magn.* 45 (10) (2009) 3919–3922.
- [18] B.V. de Wiele, A. Manzin, L. Dupré, F. Olyslager, O. Bottauscio, M. Chiampi, *IEEE Trans. Magn.* 45 (3) (2009) 1614–1617.
- [19] J.L. Blue, M.R. Scheinfein, *IEEE Trans. Magn.* 27 (6) (1991) 4778–4780.
- [20] M. Jones, J.J. Miles, *J. Magn. Magn. Mater.* 171 (1–2) (1997) 190–208.
- [21] H.N. Bertram, C. Seberino, *J. Magn. Magn. Mater.* 193 (1999) 388–394.
- [22] J. Fidler, T. Schrefl, *J. Phys. D Appl. Phys.* 33 (15) (2000) 135–156.
- [23] B. Van de Wiele, F. Olyslager, L. Dupré, *IEEE Trans. Magn.* 43 (6) (2007) 2917–2919.
- [24] D.G. Porter, M.J. Donahue, *J. Appl. Phys.* 103 (7) (2008), 07D920–07D920-3.
- [25] A. Romeo, G. Finocchio, M. Carpentieri, L. Torres, G. Consolo, B. Azzerboni, *Phys. B* 403 (2–3) (2008) 464–468.
- [26] O. Bottauscio, A. Manzin, *IEEE Trans. Magn.* 47 (5) (2011) 1154–1157.
- [27] O. Bottauscio, M. Chiampi, A. Manzin, *IEEE Trans. Magn.* 44 (11) (2008) 3149–3152.
- [28] R. Chang, M.A. Escobar, S. Li, M.V. Lubarda, V. Lomakin, *J. Appl. Phys.* 111 (2012) 3149–3152.
- [29] G. Fidler, J. Fidler, J. Lee, T. Schrefl, R.L. Stamps, H.B. Braun, D. Suess, *J. Appl. Phys.* 111 (9) (2012) 3149–3152.
- [30] S. Bartels, *Proc. Appl. Math. Mech.* 6 (2006) 19–22.
- [31] M. d'Aquino, C. Serpico, G. Miano, *J. Comput. Phys.* 209 (2) (2005) 730–753.
- [32] X.P. Wang, C.J. Garcia-Cervera, E. Weinan, *J. Comput. Phys.* 171 (2001) 357–372.
- [33] C. Garcia-Cervera, E. Weinan, *IEEE Trans. Magn.* 39 (3) (2003) 1766–1770.
- [34] W.C. Nam, M.H. Cho, Y.P. Lee, *J. Korean Phys. Soc.* 53 (3) (2008) 1626–1629.
- [35] D.R. Jeong, J.S. Kim, *J. Comput. Appl. Math.* 234 (2) (2010) 613–623.
- [36] J.S. Kim, H.O. Bae, *J. Korean Phys. Soc.* 53 (2) (2008) 672–679.
- [37] C.H. Kim, S.H. Shin, H.G. Lee, J.S. Kim, *J. Korean Phys. Soc.* 55 (4) (2009) 1451–1460.
- [38] U. Trottenberg, C. Oosterlee, A. Schüller, *Multigrid*, Academic Press, New York, 2001.
- [39] S. Bartels, J. Ko, A. Prohl, Numerical approximation of the Landau–Lifshitz–Gilbert equation and finite time blow-up of weak solutions, [Preprint]. Available: <http://stat.ethz.ch/fim/preprints/2005/prohl2.pdf>.
- [40] S. Bartels, A. Prohl, *SIAM J. Numer. Anal.* 44 (4) (2006) 1405–1419.